Research Square

Preprints are preliminary reports that have not undergone peer review.
They should not be considered conclusive, used to inform clinical practice,
or referenced by the media as validated information.

Antibacterial, antibiofilm, modulatory effects, pharmacokinetic profile, toxicity and molecular docking of Monarda fistulosa essential oil against Multidrug-Resistant Acinetobacter baumannii

Marcílio Dimateus Lima Torres Martins
Federal University of Ceará – Sobral Campus
Pedro Henrique Lima Rodrigues
Vale do Acaraú State University
Francisca Lidiane Linhares Aguiar
Vale do Acaraú State University
Geovany Amorim Gomes
Vale do Acaraú State University
Raquel Oliveira Santos Fontenelle
Vale do Acaraú State University
Francisco Cesar Barroso Barbosa
fcocesar@ufc.br
Federal University of Ceará – Sobral Campus

Research Article

Keywords: Acinetobacter baumannii, Antimicrobial resistance, Molecular docking, Monarda fistulosa, Toxicity

Posted Date: October 23rd, 2026

DOI: https://doi.org/10.21203/rs.3.rs-11133641/v1

License: This work is licensed under a Creative Commons Attribution 4.0 International License. Read Full License

Additional Declarations: No competing interests reported.

Abstract

The increasing spread of multidrug-resistant (MDR) *Acinetobacter baumannii* strains and their high biofilm-forming capacity represent a serious global public health challenge, limiting therapeutic options. Given this scenario, the aim of this study was to evaluate the chemical composition, antibacterial and antibiofilm activity, modulatory effect in combination with carbapenems and ciprofloxacin, and *in silico* interaction mechanisms of *Monarda fistulosa* essential oil (MFEO) against nosocomial isolates of MDR *A. baumannii*, as well as to predict pharmacokinetic and toxicity characteristics. Phytochemical characterization via Gas Chromatography-Mass Spectrometry (GC-MS) identified the monoterpene geraniol (92.3%) as the major constituent. Broth microdilution assays demonstrated significant antibacterial activity of MFEO, with Minimum Inhibitory Concentrations (MIC) ranging from 312 to 625 µg/mL and a bactericidal profile against all tested strains. In the synergism evaluation using the checkerboard method, MFEO exhibited an additive effect with meropenem and imipenem, reducing the carbapenem dosage required to inhibit bacterial growth in the most resistant strains, although it showed an indifferent interaction with ciprofloxacin. Furthermore, MFEO demonstrated strong dose-dependent inhibition during the initial cell adhesion phase and promoted significant eradication of pre-formed mature biofilms, outperforming meropenem control treatments at MIC, 2xMIC, and 4xMIC concentrations. *In silico* analyses indicated favorable pharmacokinetic profiles and low toxicity for the MFEO compounds, while molecular docking revealed moderate binding affinity of the compounds to the catalytic residues of OXA-24 and to the outer membrane protein A (OmpA). Taken together, these results demonstrate the potential of MFEO as a phytotherapeutic agent and as a promising adjuvant in combating severe infections caused by MDR *A. baumannii*.

1 INTRODUCTION

Acinetobacter baumannii is an aerobic Gram-negative bacterium frequently associated with various infections, such as pneumonia and bacteremia, with mortality rates ranging from 34% to 44.5% [1]. Furthermore, this species is considered a critical priority for the development of new therapeutic agents by the WHO, particularly due to its widespread antimicrobial resistance, including to carbapenem antibiotics [2]. Recent data published by the Global Burden of Disease (GBD) indicate that, in the absence of effective interventions, the number of deaths attributable to antimicrobial resistance (AMR) could reach approximately 1.91 million per year by 2050, while AMR-associated deaths could reach 8.22 million annually [3].

The resistance of *A. baumannii* is due to multiple mechanisms of action, such as modulation of outer membrane permeability, enzymatic modifications that neutralize antibiotics, development of active efflux systems, and biofilm formation [4]. Biofilms are complex biological communities formed by microorganisms and enclosed by an extracellular matrix. These communities pose a major health risk, particularly in hospital settings, as they are capable of colonizing biotic and abiotic surfaces [5]. Given this challenging scenario, novel therapeutic approaches against resistant strains have become increasingly urgent. Thus, the use of natural products rich in phytochemicals, such as essential oils—either alone or combined with antibacterials—emerges as a promising alternative to combat AMR [6].

Monarda fistulosa is an herbaceous species belonging to the Lamiaceae family, commonly known as wild bergamot. Native to North America, this species is widely used in folk medicine to treat conditions such as colds, stomachaches, headaches, and wound healing [7]. Its primary product of interest is the essential oil, rich in aromatic phytochemicals with recognized antimicrobial activity, such as geraniol, linalool, thymol, and carvacrol [8]. A study conducted by Mattarelli *et al*. [9] demonstrated that *Monarda fistulosa* essential oil (MFEO) exhibits strong antibacterial activity against the Gram-negative bacterium *Escherichia coli*. However, studies evaluating the antibacterial and antibiofilm activities of MFEO against multidrug-resistant strains of *A. baumannii* remain scarce.

Therefore, the objective of this study was to investigate the antibacterial and antibiofilm activities, as well as the synergistic potential, of MFEO, alone and in combination with carbapenems, against multidrug-resistant clinical isolates of *A. baumannii*, utilizing complementary *in vitro* and *in silico* approaches.

2 MATERIALS AND METHODS

2.1 Bacterial isolates

Five nosocomial multidrug-resistant (MDR) *A. baumannii* isolates from the biobank of the Laboratory of Microbiology and Parasitology at FAMED (UFC/Sobral) were used. The isolates were initially identified using the automated VITEK® 2 system (bioMérieux, Marcy-l'Étoile, France), and their identities were confirmed by Polymerase Chain Reaction (PCR). The susceptibility profile was also previously determined by VITEK® 2 (Table 1) and confirmed using broth microdilution assays against antibiotics from four distinct classes, namely aminoglycosides, carbapenems, fluoroquinolones, and polymyxins.

Table 1
Phenotypic antimicrobial resistance profile and OXA carbapenemase genes of multidrug-resistant *A. baumannii* clinical isolates

Acinetobacter baumannii	**Source**	**OXA gene**	**Antibiotic resistance**
AB03	Cerebrospinal fluid (CSF)	OXA-24	AMP, FEP, FOX, CAZ, CRO, CXM, CXM-AXT, CIP, GEN, IPM, MEM, TZP
AB04	Tracheal aspirate	OXA-23	AMP, SAM, FEP, FOX, CAZ, CRO, CXM, CXM-AXT, CIP, IPM, MEM, TZP
AB07	Blood	OXA-23	AMK, AMP, SAM, FEP, FOX, CAZ, CRO, CXM, CXM-AXT, CIP, GEN, IPM, MEM, TZP
AB13	Blood	OXA-24	AMP, FEP, FOX, CAZ, CRO, CXM, CXM-AXT, CIP, GEN, IPM, MEM, TZP
AB49	Urine	OXA-23/OXA-24	AMP, FEP, CRO, CXM, CXM-AXT, CIP, GEN, IPM, MEM, TZP

Legend: AMK: amikacin; AMP: ampicillin; SAM: ampicillin/sulbactam; FEP: cefepime; FOX: cefoxitin; CAZ: ceftazidime; CRO: ceftriaxone; CXM: cefuroxime; CXM-AXT: cefuroxime axetil; CIP: ciprofloxacin; GEN: gentamicin; IPM: imipenem; MEM: meropenem; TZP: piperacillin/tazobactam.

2.2 Essential oil acquisition

The volatile oil from *M. fistulosa* leaves was commercially purchased from the online store Laszlo® (Belo Horizonte, MG, Brazil), an aromatherapy company. The leaves were collected in Canada, and the oil was extracted by steam distillation.

2.3 Chemical characterization of the essential oil

The chemical composition of the essential oil was determined by gas chromatography-mass spectrometry (GC-MS) analysis using an Agilent system (model GC-7890B / MSD-5977A, quadrupole), with electron impact ionization at 70 eV, an HP-5MS methylpolysiloxane column (30 m × 0.25 mm × 0.25 µm, Agilent), and helium as carrier gas at a flow rate of 1.00 mL/min (8.8 psi) with a constant linear velocity of 36.8 cm/s. The injector temperature was set at 250°C, detector temperature at 150°C, and transfer line temperature at 280°C. Chromatographic oven temperature program: initial temperature of 70°C, with a heating ramp of 4°C/min up to 180°C, followed by an increase of 10°C/min up to 250°C by the end of the run (total run time: 34.5 min).

The various chemical constituents of MFEO were identified by visually comparing their mass spectra with literature data and spectra provided by the instrument's database (NIST version 2.0, 2012), complemented by comparing their retention indices with those reported in the literature [10]. A standard solution of *n*-alkanes was injected under the same chromatographic conditions as the sample to determine the retention indices [11]. The percentages of individual constituents were calculated using the integrated peak areas relative to the total area of all constituents in the sample.

2.4 Preparation of essential oil and antibiotics

The antibiotics gentamicin, polymyxin B, imipenem, meropenem, and ciprofloxacin were purchased from Sigma-Aldrich (St. Louis, MO, USA). Stock solutions were prepared according to the manufacturer's instructions and subjected to serial dilutions to obtain final concentrations ranging from 512 to 0.015 µg/mL, with the exception of polymyxin B, which was tested at concentrations ranging from 2 to 0.0078 µg/mL.

MFEO was prepared at a stock concentration of 10,000 µg/mL using Brain Heart Infusion (BHI) broth supplemented with 5% dimethyl sulfoxide (DMSO) and 0.5% Tween 80 to facilitate solubilization. Subsequently, serial dilutions were performed to achieve final concentrations ranging from 2,500 to 4.9 µg/mL.

2.5 Determination of minimum inhibitory concentration (MIC)

The minimum inhibitory concentration of MFEO against the isolates was determined using the broth microdilution method, as recommended by the Clinical and Laboratory Standards Institute [12].

Initially, the isolates previously reactivated in BHI broth were subcultured onto BHI agar and incubated for 24 hours at 37°C under aerobic conditions to allow colony growth. After this period, a bacterial inoculum was prepared using the McFarland standard and diluted to a final concentration of 10^6 CFU/mL. A 100 µL volume of this inoculum was added to 96-well microdilution plates following the addition of 100 µL of BHI broth and serial dilutions of MFEO ranging from 2,500 to 4.9 µg/mL. The plates were then incubated in an incubator at 37°C for 24 hours and visually evaluated for turbidity to determine the minimum inhibitory concentration (MIC), defined as the lowest concentration capable of inhibiting 100% of visible bacterial growth.

2.6 Determination of minimum bactericidal concentration (MBC)

The determination of the MBC was performed using the method described by Rodríguez-Melcón *et al*. [13]. Following MIC determination, a 100 µL aliquot from wells showing no visible microbial growth was transferred onto Petri dishes containing BHI agar, which were then incubated at 37°C for 24 hours under aerobic conditions. The MBC was defined as the lowest MFEO concentration at which no bacterial growth was observed on the inoculated agar surface (corresponding to 99.9% microbial killing).

.

2.7 Checkerboard assay

The combination between MFEO and standard antibiotics, including meropenem, imipenem, and ciprofloxacin, was evaluated using the checkerboard technique, a method used to assess compound interactions by calculating the Fractional Inhibitory Concentration Index (FICI). The FICI is calculated by adding the Fractional Inhibitory Concentration (FIC) for each tested compound, defined as the ratio between the MIC of each drug in combination and the MIC of the same drug alone [14].

The isolates showing the highest resistance to imipenem, meropenem, and ciprofloxacin were selected for this experiment. The tested products were prepared at concentrations based on their respective MIC values. Initially, 50 µL of BHI broth was added to all 96 wells of a microdilution plate. Then, 50 µL of MFEO was added to the first column, followed by serial dilutions across the plate up to the 10th column, with MFEO concentrations ranging from MIC to MIC/10. Vertically along the rows, 50 µL of imipenem was added at varying concentrations ranging from MIC to MIC/8. Finally, 100 µL of bacterial inoculum (10^6 CFU/mL) was added to all wells. BHI broth with inoculum served as the negative control, while the MICs of the standard antibiotic and MFEO evaluated separately served as positive controls. Assays were performed in duplicate. The combined effect was classified as synergistic when $FICI \leq 0.5$, additive when $0.5 < FICI \leq 1.0$, indifferent when $1.0 < FICI \leq 4.0$, and antagonistic when $FICI > 4.0$ [15].

2.8 Evaluation of antibiofilm activity

To evaluate the antibiofilm effect of MFEO during the adhesion phase and on pre-formed biofilms of *A. baumannii*, the crystal violet staining method described by Kim *et al*. [16] was used, with modifications. The most resistant isolates were selected for this analysis.

First, *A. baumannii* isolates were inoculated (1×10^6 CFU/mL) in BHI broth supplemented with 1% glucose and treated with MFEO at MIC, 2 × MIC, and 4 × MIC. Meropenem was used as the standard drug at MIC, 2 × MIC, and 4 × MIC concentrations. Afterwards, they were incubated overnight to evaluate the inhibitory effect of MFEO on biofilm formation. Following 24 h of incubation at 37°C, the culture medium was discarded, and the wells were washed three times with 200 µL of sterile Phosphate-

Buffered Saline (PBS) to remove planktonic cells. Biofilms were fixed with 200 µL of methanol for 10 min and stained with 0.1% crystal violet. After discarding the excess dye, the stained biofilms were rinsed three times with sterile deionized water, dried at 60°C for 1 h, and solubilized with 250 µL of 33% glacial acetic acid for 15 min. The solubilized biofilms were quantified by measuring absorbance at 570 nm using a microplate reader (ELISA reader).

To examine the effect of MFEO on pre-formed biofilms, 200 µL of bacterial culture diluted in medium was inoculated into 96-well plates and incubated aerobically at 37°C for 24 h to allow biofilm maturation. The wells were washed three times with PBS, and 200 µL of BHI containing MFEO (MIC, 2 × MIC, and 4 × MIC) was added to each well. After an additional 24 h incubation, the biofilms were stained and quantified as described above.

2.9 Statistical analysis

The data obtained from the antibiofilm activity assays were subjected to one-way analysis of variance (ANOVA), followed by Tukey's post hoc test for multiple comparisons, using GraphPad Prism software, version 8.0 (GraphPad Software Inc., San Diego, CA, USA). Results were expressed as mean ± standard deviation (SD), and values of $p < 0.05$ were considered statistically significant.

2.10 *In silico* assays

For the *in silico* experiments, the structures of the compounds present in MFEO were obtained from the PubChem database (https://pubchem.ncbi.nlm.nih.gov/) in canonical SMILES format. The selected compounds were geraniol (CID: 637566), nerol (CID: 643820), linalool (CID: 6549), α-terpinene (CID: 7462), and *o*-cymene (CID: 10703).

2.11 Pharmacokinetic profile prediction

The pkCSM tool (https://biosig.lab.uq.edu.au/pkcsm/prediction) was employed to predict the absorption, distribution, metabolism, and excretion (ADME) properties of MFEO phytoconstituents, providing essential data to understand how these compounds may behave in the organism [17]. Additionally, the SwissADME software (https://swissadme.ch/) was used to generate the BOILED-Egg plot, illustrating the ability of the compounds to interact with P-gp and permeate the blood-brain and gastrointestinal barriers, as well as parameters related to lipophilicity and polarity [18].

2.12 Toxicity prediction

The ProTox 3.0 web server (https://tox.charite.de/protox3/)) was used to study the toxicity profile of MFEO compounds. This software calculates predictions based on different toxicological parameters, such as organ toxicity (hepatotoxicity), oral toxicity, and toxicological endpoints (cytotoxicity, mutagenicity, carcinogenicity, and immunotoxicity) [19]. In addition to these parameters, ProTox evaluated the median lethal dose (LD_{50}) of the molecules, classifying them into six toxicity classes according to their LD_{50} values: Class I ($LD_{50} \leq 5$ mg/kg), fatal if swallowed; Class II ($5 < LD_{50} \leq 50$ mg/kg), fatal if swallowed; Class III ($50 < LD_{50} \leq 300$ mg/kg), toxic if swallowed; Class IV ($300 < LD_{50} \leq 2000$ mg/kg), harmful if swallowed; Class V ($2000 < LD_{50} \leq 5000$ mg/kg), may be harmful if swallowed; and Class VI ($LD_{50} > 5000$ mg/kg), considered relatively non-toxic in terms of acute toxicity.

2.13 Molecular docking

For molecular docking, the target proteins were the OXA-24 enzyme, the main protein responsible for carbapenem resistance in *A. baumannii*, and OmpA, one of the primary outer membrane proteins involved in *A. baumannii* biofilm formation. The three-dimensional structures of the proteins were retrieved from the RCSB Protein Data Bank (PDB) database under the identification codes (PDB ID): 3ZNT for OXA-24 and 3TD4 for OmpA. Protein structures were evaluated and prepared for docking using AutoDockTools. Preparation included the removal of water molecules and native ligands from the 3D structures, as well as the addition of Gasteiger charges and polar hydrogens [20].

MFEO compounds were used as ligands, obtained in 3D format from the PubChem database. Ligand preparation was carried out in AutoDockTools, including the addition of hydrogens, assignment of partial Gasteiger charges, and identification of rotatable bonds (torsional degrees of freedom).

To validate the docking protocol, the Root Mean Square Deviation (RMSD) was evaluated for both receptor proteins by re-docking the co-crystallized ligand into the active site. An RMSD < 2.0 was considered satisfactory for subsequent analyses, as described by Zaman *et al*. [21].

Docking was performed using AutoDock Vina software, one of the most widely used tools in *in silico* structural experiments. For molecular docking, the grid box for OXA-24 and OmpA was defined based on the location of the crystallographic ligand present in the structure obtained from the PDB. The grid box center for OXA-24 was set at coordinates x = 105.341, y = 32.851, and z = 27.047, with dimensions of 15.0 Å × 15.0 Å × 15.0 Å. For OmpA, the grid box was centered at coordinates x = 20.489, y = 2.091, and z = 27.863, with dimensions of 15.0 Å × 15.0 Å × 15.0 Å, both with an exhaustiveness parameter of 32 to intensify the search for optimal conformations. The conformation with the most favorable binding energy (in kcal/mol) was selected for further analysis.

Analyses included the evaluation of key ligand-receptor interactions, such as hydrogen bonds and electrostatic interactions. ChimeraX and Discovery Studio Visualizer software were used for visual analysis.

3 RESULTS

3.1 Chemical characterization of the essential oil

Chemical characterization of MFEO identified 5 volatile compounds (Table 2), with a predominance of oxygenated monoterpenes, including linalool, nerol, and geraniol, accounting for 98.74%; whereas the remaining 1.25% corresponded to the monoterpene hydrocarbons α-terpinene, and *o*-cymene. Among all compounds, the oxygenated monoterpene geraniol stood out, accounting for 92.3% of the total composition and thus constituting the major component.

Table 2
Phytochemical composition of MFEO

Constituents	**RI Lit**	**RI Calc**	**%**
Monoterpene Hydrocarbons			**1.25**
α-Terpinene	1017	1025	0.72
o-Cymene	1026	1038	0.53
Oxygenated Monoterpenes			**98.74**
Linalool	1096	1105	2.68
Nerol	1229	1236	3.76
Geraniol	1252	1265	92.3
TOTAL			99.99

RI Lit: Retention Index obtained from the literature (Adams, 2017); RI Calc: Calculated Retention Index; %: percentage of identified components.

3.2 Susceptibility profile of bacterial isolates

The susceptibility profile of nosocomial *A. baumannii* isolates to the antibiotics gentamicin, imipenem, meropenem, ciprofloxacin, and polymyxin B was analyzed by broth microdilution. Isolates AB13 and AB49 were overall the most resistant, with MIC values ranging from 64 to 128 µg/mL for carbapenems and ciprofloxacin, in addition to MIC > 512 µg/mL for gentamicin. All results are presented in Table 3.

Table 3
Susceptibility profile of the 5 nosocomial *A. baumannii* isolates

Isolates	Aminoglycoside		Carbapenems				Fluoroquinolone		Polymyxin	
	Gentamicin (µg/ml)		Imipenem (µg/ml)		Meropenem (µg/ml)		Ciprofloxacin (µg/ml)		Polymyxin B (µg/ml)	
	MIC	MBC	MIC	MBC	MIC	MBC	MIC	MBC	MIC	MBC
AB03	256	256	0.25	0.5	0.625	1.25	0.0625	0.0625	0.0625	0.5
AB04	1	1	0.0625	0.0625	0,031	1	0.0097	0.039	0.0625	0.25
AB07	512	> 512	1	4	0.625	1	64	256	0.0625	0.25
AB13	> 512	> 512	128	512	64	512	16	64	0.015	0.25
AB49	> 512	> 512	128	256	128	128	32	32	0.015	0.015

3.3 MIC and MBC of the essential oil

Evaluation of the antibacterial activity of MFEO demonstrated effectiveness against all five nosocomial *A. baumannii* isolates, with MIC values ranging from 312 to 625 µg/mL. Furthermore, it exhibited a bactericidal effect against all analyzed isolates (MBC/MIC ≤ 4) (Table 4).

Table 4
MIC, MBC, and MBC/MIC ratio values of MFEO against five nosocomial *A. baumannii* isolates

Isolates	MIC (µg/mL)	MBC (µg/mL)	MBC/MIC ratio
AB03	625	1,250	2
AB04	625	2,500	4
AB07	625	625	1
AB13	312	312	1
AB49	312	1.250	4

3.4 Checkerboard assay

Evaluation of the synergistic potential of MFEO in combination with the antibiotics imipenem, meropenem, and ciprofloxacin showed that MFEO exhibited a stronger effect when combined with carbapenems than with ciprofloxacin (Table 5). The combination of MFEO with carbapenems potentiated the activity of these antibiotics, reducing MIC values by 4- to 16-fold, as observed for the combination of MFEO and meropenem against isolate AB13.

Table 5
FICI values of MFEO combinations with imipenem, meropenem, and ciprofloxacin

Imipenem						
Isolate	**MIC MFEO alone**	**MIC MFEO combined**	**MIC imipenem alone**	**MIC imipenem combined**	**FICI**	**Interpretation**
AB13	312	156	128	32	0.75	Additive
AB49	312	156	128	64	1.00	Additive
Meropenem						
Isolate	**MIC MFEO alone**	**MIC MFEO combined**	**MIC meropenem alone**	**MIC meropenem combined**	**FICI**	**Interpretation**
AB13	312	156	64	4	0.56	Additive
AB49	312	156	128	32	0.75	Additive
Ciprofloxacin						
Isolate	**MIC MFEO alone**	**MIC MFEO combined**	**MIC ciprofloxacin alone**	**MIC ciprofloxacin combined**	**FICI**	**Interpretation**
AB13	312	156	16	16	1.5	Indifferent
AB49	312	156	32	32	1.5	Indifferent

3.5 Evaluation of antibiofilm activity

Figure 1 shows that during the biofilm adhesion phase of isolate AB13, all tested concentrations of MFEO inhibited approximately 100% of biofilm formation. In contrast, meropenem reduced biofilm formation by only 6.9% at MIC, showing no statistically significant difference compared to the control, whereas at 2×MIC and 4×MIC concentrations, it achieved reductions of 71.3% and 95.7%, respectively.

In the mature biofilm of isolate AB13, MFEO activity was also substantial, reducing biomass by 45%, 68.9%, and 78.8% at concentrations corresponding to MIC, 2×MIC, and 4×MIC, respectively. At this same biofilm stage, meropenem reduced biomass by 8.2% at MIC (without statistical significance compared to the control), 44.5% at 2×MIC, and 55.4% at 4×MIC (Fig. 1).

Regarding the biofilm of isolate AB49 during the adhesion stage, MFEO promoted a reduction greater than 96% across all tested concentrations. Treatment with meropenem suppressed biofilm formation by 81.8% under exposure to MIC, 97.4% at 2×MIC, and 97.6% at 4×MIC (Fig. 1).

In the mature biofilm of isolate AB49, MFEO also demonstrated relevant antibiofilm activity, reducing biomass by 70.1%, 76.5%, and 75.6% at concentrations corresponding to MIC, 2×MIC, and 4×MIC, respectively. At this same stage, meropenem showed a reduction of only 14.5% at MIC, while at 2×MIC and 4×MIC concentrations, it achieved reductions of 73.7% and 76.8%, respectively (Fig. 1).

3.6 Pharmacokinetic profile of MFEO compounds

The ADMET parameters of the MFEO compounds (Table 6) indicate good Caco-2 permeability (log Papp > 0.90), satisfactory intestinal absorption (> 30%), and the ability to cross the blood-brain barrier (BBB) (log BB > 0.3). Additionally, all compounds exhibited an adequate steady-state volume of distribution (VDss > 0.71), suggesting favorable systemic distribution.

None of the compounds were predicted to act as substrates or inhibitors of cytochrome P450 (CYP) enzymes, with the exception of *o*-cymene, which was flagged as a CYP1A2 inhibitor. Regarding excretion, no compound served as a renal substrate for the OCT2 transporter. Finally, the toxicity evaluation—assessed via the Ames test, hERG channel inhibition, skin

sensitization, and hepatotoxicity—indicated a low overall toxicological risk, although geraniol, nerol, linalool, and *o*-cymene were predicted as skin sensitizers.

Table 6
Pharmacokinetic properties of MFEO compounds

	Geraniol	Nerol	Linalool	α-terpinene	*o*-cymene	Unit / type
			Absorption			
Water solubility	-2.679	-2.866	-2.612	-3.941	-4.113	log mol/L
Caco-2 permeability	1.365	1.490	1.493	1.414	1.526	log Papp (10^{-6} cm/s)
Intestinal absorption	95.906	92.788	93.163	96.219	93.882	% Absorbed
Skin permeability e	-1.689	-1.511	-1.737	-1.489	-1.178	log Kp
P-gp substrate	yes	no	no	no	no	Categorical (Yes/No)
P-gp I/II inhibitor	no	no	no	no	no	Categorical (Yes/No)
			Distribution			
VDss (human)	0.170	0.170	0.152	0.372	0.744	log L/kg
Fraction unbound	0.447	0.447	0.484	0.502	0.162	Fu
BBB permeability	0.606	0.606	0.598	0.736	0.480	log BB
CNS permeability	-2.159	-2.159	-2.339	-2.324	-1.397	log PS
			Metabolism			
CYP2D6 substrate	no	no	no	no	no	Categorical (Yes/No)
CYP3A4 substrate	no	no	no	no	no	Categorical (Yes/No)
CYP1A2 inhibitor	no	no	no	no	yes	Categorical (Yes/No)
CYP2C19 inhibitor	no	no	no	no	no	Categorical (Yes/No)
CYP2C9 inhibitor	no	no	no	no	no	Categorical (Yes/No)
CYP2D6 inhibitor	no	no	no	no	no	Categorical (Yes/No)
CYP3A4 inhibitor	no	no	no	no	no	Categorical (Yes/No)
			Excretion			
Total clearance	0.437	0.437	0.446	0.223	0.259	log mL/min/kg
Renal OCT2 substrate	no	no	no	no	no	Categorical (Yes/No)
			Toxicity			
Ames toxicity	no	no	no	no	no	Categorical (Yes/No)
hERG I/II inhibitors	no	no	no	no	no	Categorical (Yes/No)
Skin sensitization	yes	yes	yes	no	yes	Categorical (Yes/No)
Hepatotoxicity	no	no	no	no	no	Categorical (Yes/No)

The BOILED-Egg plot (Fig. 2), generated using SwissADME, demonstrated that all compounds exhibit high human intestinal absorption (white region) and the potential to cross the blood-brain barrier (BBB) (yellow region). Furthermore, it indicated that none of the molecules are substrates for P-glycoprotein (P-gp) (red dots).

3.7 Toxicity evaluation

The toxicity evaluation of the MFEO compounds performed using ProTox revealed that none of the compounds were predicted to be hepatotoxic, exhibiting high probability scores ranging from 0.76 to 0.87 (Table 7). Regarding other toxicological endpoints, all compounds were classified as non-toxic, with the exception of *o*-cymene, for which the software indicated potential carcinogenicity (confidence score of 0.64).

Additionally, the software-predicted LD50 values ranged from 1,370 to 2,200 mg/kg. All compounds were assigned to toxicity Class V, except for α-terpinene and *o*-cymene, which were categorized under Class IV.

Table 7
Toxicity profile of MFEO compounds

Compound	Hepatotoxicity		Carcinogenicity		Cytotoxicity		Immunotoxicity		Mutagenicity		Predicted LD50 (mg/kg)	Toxicity Class
	Pr	Pb	Pr	Pb	Pr	Pb	Pr	Pb	Pr	Pb		
Geraniol	NH	0.79	NC	0.76	NC	0.85	NI	0.99	NM	0.97	2,100	V
Nerol	NH	0.79	NC	0.76	NC	0.85	NI	0.99	NM	0.97	2,100	V
Linalool	NH	0.76	NC	0.64	NC	0.82	NI	0.99	NM	0.95	2,200	V
α-terpineno	NH	0.78	NC	0.75	NC	0.85	NI	0.95	NM	0.85	1,680	IV
o-cimeno	NH	0.87	C	0.64	NC	0.86	NI	0.99	NM	0.86	1,370	IV

Legend: Pred: Prediction; Prob: Prediction probability; NH: Non-hepatotoxic; NC: Non-carcinogenic; C: Carcinogenic; NI: Non-immunotoxic; NM: Non-mutagenic; LD50: Median lethal dose (mg/kg).

3.8 Molecular docking

The redocking protocol for the OXA-24 enzyme yielded an RMSD value of 1.367 Å, falling within the acceptable threshold (RMSD < 2 Å). The binding energy between the MFEO compounds and the OXA-24 enzyme ranged from − 4.552 to -4.819 kcal/mol, with geraniol exhibiting the most favorable binding affinity, while *o*-cymene presented the least favorable value (Table 8).

Table 8
Binding energy values (kcal/mol) of MFEO monoterpenes interacting with OXA-24 and OmpA targets

Ligantes	OXA-24 (Kcal/mol)	OmpA (Kcal/mol)
Geraniol	− 4.819	− 4.492
Nerol	− 4.806	− 4.679
o-Cymene	− 4.552	− 4.218
α-Terpinene	− 4.750	− 4.672
Linalool	− 4.791	− 4.551

The main interactions between the ligands and OXA-24 included van der Waals forces, alkyl interactions, and hydrogen bonds, specifically involving geraniol with the serine 128 (Ser 128) residue, and nerol with the serine 219 (Ser 219) and lysine 218 (Lys 218) residues (Fig. 3). In contrast, the minor compounds *o*-cymene, α-terpinene, and linalool exhibited predominantly van der Waals and alkyl interactions, engaging with several amino acid residues such as Ser 219, Ser 128, and tyrosine 112 (Tyr 112).

In the evaluation with the OmpA enzyme, the RMSD was 1.425 Å, validating the docking protocol. Binding energies with the OmpA enzyme ranged from − 4.218 to -4.679 kcal/mol. The compound with the most favorable binding value was nerol (-4.679

kcal/mol), whereas *o*-cymene showed the lowest binding affinity (Table 9).

In Fig. 4, the main interactions between MFEO compounds and the OmpA enzyme were hydrogen bonds, hydrophobic interactions, and Pi-alkyl/Pi-anion interactions, alongside a few unfavorable interactions. The primary protein residues involved in these interactions included asparagine 237 (Asn 237), aspartic acid 271 (Asp 271), leucine 282 (Leu 282), threonine 236 (Thr 236), and arginine 329 (Arg 329). Furthermore, hydrogen bonds involving Asn 279 and Asp 271 with nerol were prominent, making it the compound that established the greatest number of such bonds.

4 DISCUSSION

The present study demonstrated a phytochemical profile predominantly dominated by oxygenated monoterpenes, a finding supported by previous literature. Ghosh *et al*. [22] demonstrated that MFEO extracted from leaves is also predominantly composed of oxygenated monoterpenes (77.7%), reinforcing the results of the current work. However, unlike the major compound identified in this study (geraniol), the predominant molecule in the aforementioned study was carvacrol, accounting for 71.5% of the total composition.

Traditionally, the MFEO chemotype is classified into two main groups dominated by thymol and carvacrol. However, alternative major compounds, such as geraniol and linalool, have been identified in recent analyses [23]. Highlighting the existence of different chemotypes, Gontar *et al*. [24] characterized the phytochemical profile of MFEO across different plant developmental stages, finding carvacrol as the dominant compound in some stages and *p*-cymene in others.

Variations in essential oil phytochemical composition can result from several well-documented factors, including harvest date, season, time of day, as well as the methods used for plant material collection and essential oil extraction [25].

A literature review revealed no previous studies assessing the activity of MFEO against *A. baumannii*, highlighting the novelty of this work. Nevertheless, its efficacy against other Gram-negative bacterial species has been reported. Mattarelli *et al*. [9] demonstrated that MFEO harvested in two different periods exhibited activity against *E. coli*, with MIC values ranging from 0.25% to 1.00%, while also displaying a bactericidal effect, with the MBC value equal to the MIC. Notably, the MFEO in the present study also displayed a bactericidal effect, as defined by an MBC value equal to or less than 4-fold the MIC [26].

Conversely, Aguiar *et al*. [27] reported high MIC values (ranging from 4,000 to 8,000 µg/mL) against *E. coli* and *K. pneumoniae* strains. This discrepancy may be attributed to variations in intrinsic susceptibility among bacterial species, as well as methodological differences between assays.

Most bactericidal molecules target multiple cellular structures, suggesting that the compounds present in MFEO act through diverse mechanisms of action [28].

Geraniol, the major compound of MFEO in this study, was evaluated both in its pure form and in nanoemulsions by Feng *et al*. [29] against various bacteria, including *S. aureus*, *E. coli*, and *Salmonella typhimurium*. Their findings demonstrated that geraniol nanoemulsions exhibited superior antibacterial activity compared to pure geraniol, with MIC values ranging from 3.9 to 7.8 µL/mL. These findings suggest that nanostructured formulations containing MFEO could potentially enhance its antibacterial activity further.

The combined effect of MFEO and conventional antibiotics was evaluated using the checkerboard assay, which can reveal synergistic, additive, or indifferent interactions. Although the combination of MFEO with carbapenems did not display synergy in this study, it exhibited an additive effect, significantly reducing the MICs of the antibiotics against the tested strains. Additive interactions, such as those observed here, indicate that the antibacterial activities of the natural product and the antibiotic contribute independently to overall activity, leading to lower MIC values [30].

Several studies have highlighted potential mechanisms through which essential oils (EOs) can potentiate or restore the efficacy of conventional antibiotics. These include altering bacterial membrane permeability to increase antibiotic uptake, directly inhibiting enzymes such as β-lactamases, and modulating efflux pumps to reverse antimicrobial resistance [31]. Furthermore,

literature indicates that such combinations can induce structural damage to the cell wall and membrane, leading to leakage of proteins and nucleic acids [32].

Conversely, this potentiating effect was not observed when MFEO was combined with ciprofloxacin. The interaction between MFEO and ciprofloxacin was indifferent, failing to enhance antibacterial activity. Previous research indicates that indifferent outcomes in natural product–antibiotic combinations can stem from various factors, including essential oil chemotypes and specific phenotypic characteristics of the bacterial strain influencing ciprofloxacin susceptibility [33].

MFEO demonstrated significant antibiofilm activity, particularly during the adhesion phase. Biofilms in the initial adhesion phase are generally more susceptible to antibacterial agents because the extracellular polymeric substance (EPS) matrix is poorly developed at this stage, offering minimal resistance to antibiofilm compounds [34].

Furthermore, MFEO effectively reduced the biomass of mature biofilms, which typically exhibit heightened resistance to antimicrobial agents due to the presence of a complex extracellular matrix, thereby emphasizing the antibiofilm potential of MFEO. Overall, the antibiofilm activity of MFEO exhibited dose-dependent behavior, with stronger effects observed at higher concentrations.

To date, no studies in the literature have evaluated the antibiofilm activity of MFEO against *A. baumannii* biofilms. However, studies investigating terpene-rich EOs have reported substantial antibiofilm efficacy. Tapia-Rodriguez *et al*. [35] demonstrated that *Lippia graveolens* essential oil and its primary constituents, carvacrol and thymol, significantly reduced *A. baumannii* biofilm biomass in a concentration-dependent manner. These findings align with and reinforce the present results, highlighting the antibiofilm potential of terpene compounds.

In silico pharmacokinetic predictions showed that all compounds present in MFEO exhibit high oral absorption rates, suggesting favorable potential for future oral formulations. A study by Pavan *et al*. [36] supports these findings; their *in vivo* experiments with geraniol (the major compound in MFEO) demonstrated high intestinal absorption and BBB penetration. Additionally, they reported that geraniol exhibits low toxicity even at high concentrations, directly corroborating our findings.

Moreover, additional toxicity assessments performed using ProTox 3.0 reinforced the pkCSM predictions, indicating that none of the compounds possess hepatotoxic potential. Furthermore, safety profile evaluations considered additional parameters, including mutagenicity, immunotoxicity, cytotoxicity, and carcinogenicity [37]. Across all parameters, ProTox predictions classified the MFEO compounds as non-toxic, underscoring the pharmacological potential of MFEO and highlighting the need for future *in vitro* and *in vivo* studies to validate these findings.

In addition to these data, ProTox 3.0 estimated the LD50 values of the compounds (i.e., the predicted dose required to kill 50% of test organisms) and categorized them into six acute systemic toxicity classes. Geraniol, nerol, and linalool were assigned to toxicity Class V (substances that may be harmful if swallowed), whereas α-terpinene and *o*-cymene were classified under Class IV (harmful if swallowed).

ProTox 3.0 is a widely used, free web server based on molecular similarity and machine learning, capable of predicting up to 61 toxicity endpoints. Its application in natural product research, such as MFEO screening, is highly relevant as it streamlines early-stage drug discovery, reduces costs, and provides reliable predictions during initial screening phases [38].

None of the compounds violated Lipinski's rule of five, emphasizing their drug-like pharmacological potential. Mohamed *et al.* [39] evaluated the drug-likeness of geraniol using the same software and demonstrated that geraniol complied fully with Lipinski's rule of five, consistent with our findings.

Although the molecular interactions between MFEO compounds and the OXA-24 enzyme yielded modest binding energy values (-4.552 to -4.819 kcal/mol), several key interactions were identified, particularly hydrogen bonds formed by geraniol and nerol with residues in the catalytic pocket. Hydrogen bonds play a pivotal role in stabilizing ligand–receptor binding [40].

The interactions between MFEO compounds and catalytic pocket residues, such as tyrosine 112 (Tyr 112), methionine 223 (Met 223), and serine 81 (Ser 81), are particularly notable. Studies suggest that Tyr 112 and Met 223 form an essential hydrophobic

bridge required for accommodating carbapenem substrates [41]. This implies that interactions between MFEO compounds and these key residues could impact carbapenemase enzyme activity.

Additional molecular docking was performed against OmpA, a prominent outer membrane porin and major virulence factor in *A. baumannii* that plays a central role in cell adhesion, biofilm assembly, and maintenance [42]. Calculated binding energies for OmpA demonstrated satisfactory affinity for MFEO monoterpenes (-4.218 to -4.679 kcal/mol), with nerol (-4.679 kcal/mol) and linalool (-4.672 kcal/mol) showing the highest binding affinities.

Highlighting the significance of targeting OmpA, Singothu *et al*. [43]conducted a virtual screening combining molecular docking and molecular dynamics to identify potential inhibitors from a natural product database containing over 100,000 compounds.

Given the key role of OmpA in bacterial adhesion and biofilm development, the interactions observed between MFEO compounds and this protein may help explain the antibiofilm effects demonstrated in the *in vitro* experiments.

Although the findings of the present study are promising and encouraging, it is important to highlight its limitations. Among these are the small number of strains analyzed, which may impact the reproducibility of the results, and the need for *in vivo* toxicity studies to ensure the safety of MFEO.

5 CONCLUSION

Based on the results of the present study, it can be concluded that MFEO, specifically the chemotype with geraniol as its major compound, possesses relevant antibacterial activity against MDR nosocomial *A. baumannii* strains, demonstrating bactericidal activity. Furthermore, when combined with imipenem and meropenem, MFEO significantly reduced the MIC of these antibiotics, partially restoring the susceptibility of *A. baumannii* strains to carbapenems. The antibiofilm activity of MFEO during both the adhesion phase and in mature biofilms was also substantial, proving superior to that of meropenem.

In silico evaluation indicated a low toxicological risk for MFEO molecules. Additionally, the pharmacokinetic profile was satisfactory, highlighting a pharmacological potential that should be further validated through *in vitro* and *in vivo* experiments. Finally, molecular docking conducted with the OXA-24 and OmpA enzymes revealed favorable binding energies between MFEO compounds and target proteins.

Overall, this study provides novel findings regarding the antibacterial efficacy of MFEO against MDR *A. baumannii* in both planktonic and sessile forms, alongside key pharmacokinetic and molecular docking insights to guide future investigations.

Declarations

Funding

This study was supported in part by the Coordenação de Aperfeiçoamento de Pessoal de Nível Superior - Brasil (CAPES).

Competing Interests

The authors have no relevant financial or non-financial interests to disclose.

Data Availability

The datasets generated during and/or analyzed during the current study are available from the corresponding author on reasonable request.

Author Contributions

Marcílio Dimateus Lima Torres Martins, Pedro Henrique Lima Rodrigues, Francisca Lidiane Linhares de Aguiar, and Geovany Amorim Gomes carried out the laboratory experiments, in silico analyses, and data collection. Francisco Cesar Barroso Barbosa

and Raquel Oliveira Santos Fontenelle supervised the study, provided overall guidance, and critically revised the manuscript. All authors read and approved the final manuscript.

References

1. Sarshar M, Behzadi P, Scribano D et al (2021) Acinetobacter baumannii: An Ancient Commensal with Weapons of a Pathogen. Pathogens 10:387. https://doi.org/10.3390/pathogens10040387
2. Boral J, Pınarlık F, Ekinci G et al (2023) Does Emerging Carbapenem Resistance in Acinetobacter baumannii Increase the Case Fatality Rate? Systematic Review and Meta-Analysis. Infect Disease Rep 15:564–575. https://doi.org/10.3390/idr15050055
3. Naghavi M, Vollset SE, Ikuta KS et al (2024) Global burden of bacterial antimicrobial resistance 1990–2021: a systematic analysis with forecasts to 2050. Lancet 404:1199–1226. https://doi.org/10.1016/S0140-6736(24)01867-1
4. Kyriakidis I, Vasileiou E, Pana ZD, Tragiannidis A (2021) Acinetobacter baumannii Antibiotic Resistance Mechanisms. Pathogens 10:373. https://doi.org/10.3390/pathogens10030373
5. Mishra A, Aggarwal A, Khan F (2024) Medical Device-Associated Infections Caused by Biofilm-Forming Microbial Pathogens and Controlling Strategies. Antibiotics 13:623. https://doi.org/10.3390/antibiotics13070623
6. Raikwar G, Kumar D, Mohan S, Dahiya P (2024) Synergistic potential of essential oils with antibiotics for antimicrobial resistance with emphasis on mechanism of action: A review. Biocatal Agric Biotechnol 61:103384. https://doi.org/10.1016/j.bcab.2024.103384
7. Shanaida M, Hudz N, Jasicka-Misiak I, Wieczorek PP (2021) Polyphenols and Pharmacological Screening of a Monarda fistulosa L. dry Extract Based on a Hydrodistilled Residue By-Product. Front Pharmacol 12:563436. https://doi.org/10.3389/fphar.2021.563436
8. Malankina EL, Kuzmenko AN, Zaitchik, BTs et al (2020) Content and Composition of Wild Bergamot (Monarda fistulosa L.) Essential Oil at Different Phenological Phases. Mosc Univ Chem Bull 75:391–394. https://doi.org/10.3103/S0027131420060140
9. Mattarelli P, Epifano F, Minardi P et al (2017) Chemical Composition and Antimicrobial Activity of Essential Oils from Aerial Parts of *Monarda didyma* and *Monarda fistulosa* Cultivated in Italy. J Essent Oil Bearing Plants 20:76–86. https://doi.org/10.1080/0972060X.2016.1278184
10. Adams RP (2007) Identification of essential oil components by gas chromatography mass spectroscopy. Allured Publishing Corporation, Carol Stream, Ill
11. Van Den Dool H, Dec. Kratz P (1963) A generalization of the retention index system including linear temperature programmed gas—liquid partition chromatography. J Chromatogr A 11:463–471. https://doi.org/10.1016/S0021-9673(01)80947-X
12. Clinical and Laboratory Standards Institute (2024) Methods for Dilution Antimicrobial Susceptibility Tests for Bacteria That Grow Aerobically, 12th edn. Clinical and Laboratory Standards Institute
13. Rodríguez-Melcón C, Alonso-Calleja C, García-Fernández C et al (2021) Minimum Inhibitory Concentration (MIC) and Minimum Bactericidal Concentration (MBC) for Twelve Antimicrobials (Biocides and Antibiotics) in Eight Strains of Listeria monocytogenes. Biology 11:46. https://doi.org/10.3390/biology11010046
14. Meletiadis J, Pournaras S, Roilides E, Walsh TJ (2010) Defining Fractional Inhibitory Concentration Index Cutoffs for Additive Interactions Based on Self-Drug Additive Combinations, Monte Carlo Simulation Analysis, and *In Vitro - In Vivo* Correlation Data for Antifungal Drug Combinations against *Aspergillus fumigatus*. Antimicrob Agents Chemother 54:602–609. https://doi.org/10.1128/AAC.00999-09
15. Odds FC (2003) Synergy, antagonism, and what the chequerboard puts between them. J Antimicrob Chemother 52:1–1. https://doi.org/10.1093/jac/dkg301
16. Kim H-R, Shin D-S, Jang H-I, Eom Y-B (2020) Anti-biofilm and anti-virulence effects of zerumbone against Acinetobacter baumannii. Microbiology 166:717–726. https://doi.org/10.1099/mic.0.000930

17. Pires DEV, Blundell TL, Ascher DB (2015) pkCSM: PredictingSmall-Molecule Pharmacokinetic andToxicity Properties Using Graph-Based Signatures. J Med Chem 58:4066–4072. https://doi.org/10.1021/acs.jmedchem.5b00104
18. Rauf A, Khan H, Khan M et al (2023) In Silico, SwissADME, and DFT Studies of Newly Synthesized Oxindole Derivatives Followed by Antioxidant Studies. J Chem 2023:1–16. https://doi.org/10.1155/2023/5553913
19. Azzouni D, Alaoui Mrani S, Bahij F et al (2025) Comprehensive Phytochemical, Antioxidant, and Antibacterial Analysis of Vitex agnus-castus L. Essential Oil (VACEO): Insights from ADMET and Molecular Docking Studies. Pharmaceuticals 18:462. https://doi.org/10.3390/ph18040462
20. Morris GM, Huey R, Lindstrom W et al (2009) AutoDock4 and AutoDockTools4: Automated docking with selective receptor flexibility. J Comput Chem 30:2785–2791. https://doi.org/10.1002/jcc.21256
21. Zaman A, Noor S, Ahmad I et al (2025) Exploring cotton plant compounds for novel treatments against brain-eating Naegleria fowleri: An In-silico approach. PLoS ONE 20:e0319032. https://doi.org/10.1371/journal.pone.0319032
22. Ghosh M, Schepetkin IA, Özek G et al (2020) Essential Oils from Monarda fistulosa: Chemical Composition and Activation of Transient Receptor Potential A1 (TRPA1) Channels. Molecules 25:4873. https://doi.org/10.3390/molecules25214873
23. Keefover-Ring K (2022) The chemical biogeography of a widespread aromatic plant species shows both spatial and temporal variation. Ecol Evol 12. https://doi.org/10.1002/ece3.9265. ece3.9265
24. Gontar Ł, Geszprych A, Sitarek-Andrzejczyk M, Osińska E (2024) Influence of Plant Phenology on Chemical Composition of Monarda fistulosa L. Organs and their Bioactive Properties. Plant Foods Hum Nutr 79:920–925. https://doi.org/10.1007/s11130-024-01238-y
25. Liao Z, Huang Q, Cheng Q et al (2021) Seasonal Variation in Chemical Compositions of Essential Oils Extracted from Lavandin Flowers in the Yun-Gui Plateau of China. Molecules 26:5639. https://doi.org/10.3390/molecules26185639
26. Vaisbourd E, Glass DS, Yang Y et al (2025) Principles of bacteriostatic and bactericidal antibiotics at subinhibitory concentrations. mBio 16:e02066–e02025. https://doi.org/10.1128/mbio.02066-25
27. Aguiar CER, Cavalcante RMB, Da Silva FF et al (2026) Chemical Characterization and Antimicrobial Screening of Commercial Volatile Oils and Evaluation of the Combinatorial Effect of Patchouli Oil and Patchoulol with β-Lactams. Rev Bras Farmacogn 36:74. https://doi.org/10.1007/s43450-026-00777-6
28. Maillard J-Y, Pascoe M (2024) Disinfectants and antiseptics: mechanisms of action and resistance. Nat Rev Microbiol 22:4–17. https://doi.org/10.1038/s41579-023-00958-3
29. Feng X, Feng K, Zheng Q et al (2022) Preparation and characterization of geraniol nanoemulsions and its antibacterial activity. Front Microbiol 13:1080300. https://doi.org/10.3389/fmicb.2022.1080300
30. Nikolic I, Vukovic D, Gavric D et al (2022) An Optimized Checkerboard Method for Phage-Antibiotic Synergy Detection. Viruses 14:1542. https://doi.org/10.3390/v14071542
31. Zai MJ, Cock IE, Cheesman MJ (2025) Plant Metabolites as Potential Agents That Potentiate or Block Resistance Mechanisms Involving β-Lactamases and Efflux Pumps. IJMS 26:5550. https://doi.org/10.3390/ijms26125550
32. Sodéré P, Somda M, Zongo L et al (2025) Synergy and Mechanism of the Action of the Combination of Essential Oils and Antibiotics Against Antibiotic-Resistant Food Borne Disease Bacteria in Burkina Faso. IDR Volume 18:2743–2763. https://doi.org/10.2147/IDR.S518717
33. Neagu R, Popovici V, Ionescu L-E et al (2024) Phytochemical Screening and Antibacterial Activity of Commercially Available Essential Oils Combinations with Conventional Antibiotics against Gram-Positive and Gram-Negative Bacteria. Antibiotics 13:478. https://doi.org/10.3390/antibiotics13060478
34. Fu J, Zhang Y, Lin S et al (2021) Strategies for Interfering With Bacterial Early Stage Biofilms. Front Microbiol 12:675843. https://doi.org/10.3389/fmicb.2021.675843
35. Tapia-Rodriguez MR, Cantu-Soto EU, Vazquez-Armenta FJ et al (2023) Inhibition of Acinetobacter baumannii Biofilm Formation by Terpenes from Oregano (Lippia graveolens) Essential Oil. Antibiotics 12:1539. https://doi.org/10.3390/antibiotics12101539
36. Pavan B, Dalpiaz A, Marani L et al (2018) Geraniol Pharmacokinetics, Bioavailability and Its Multiple Effects on the Liver Antioxidant and Xenobiotic-Metabolizing Enzymes. Front Pharmacol 9:18. https://doi.org/10.3389/fphar.2018.00018

37. Lee H, Kim J, Kim J-W, Lee Y (2025) Recent advances in AI-based toxicity prediction for drug discovery. Front Chem 13:1632046. https://doi.org/10.3389/fchem.2025.1632046
38. Banerjee P, Kemmler E, Dunkel M, Preissner R (2024) ProTox 3.0: a webserver for the prediction of toxicity of chemicals. Nucleic Acids Res 52:W513–W520. https://doi.org/10.1093/nar/gkae303
39. Mohamed ME, Elmorsy MA, Younis NS (2022) Renal Ischemia/Reperfusion Mitigation via Geraniol: The Role of Nrf-2/HO-1/NQO-1 and TLR2,4/MYD88/NFκB Pathway. Antioxidants 11:1568. https://doi.org/10.3390/antiox11081568
40. Bulusu G, Desiraju GR (2020) Strong and Weak Hydrogen Bonds in Protein–Ligand Recognition. J Indian Inst Sci 100:31–41. https://doi.org/10.1007/s41745-019-00141-9
41. Mitchell JM, June CM, Baggett VL et al (2022) Conformational flexibility in carbapenem hydrolysis drives substrate specificity of the class D carbapenemase OXA-24/40. J Biol Chem 298:102127. https://doi.org/10.1016/j.jbc.2022.102127
42. Oh MH, Islam MM, Kim N et al (2025) AbOmpA in Acinetobacter baumannii: exploring virulence mechanisms of outer membrane-integrated and outer membrane vesicle-associated AbOmpA and developing anti-infective agents targeting AbOmpA. J Biomed Sci 32:53. https://doi.org/10.1186/s12929-025-01147-5
43. Singothu S, Devsani N, Jahidha Begum P et al (2024) Molecular docking and molecular dynamics studies of natural products unravel potential inhibitors against OmpA of *Acinetobacter baumannii*. J Biomol Struct Dynamics 42:9064–9075. https://doi.org/10.1080/07391102.2023.2250446

Figures

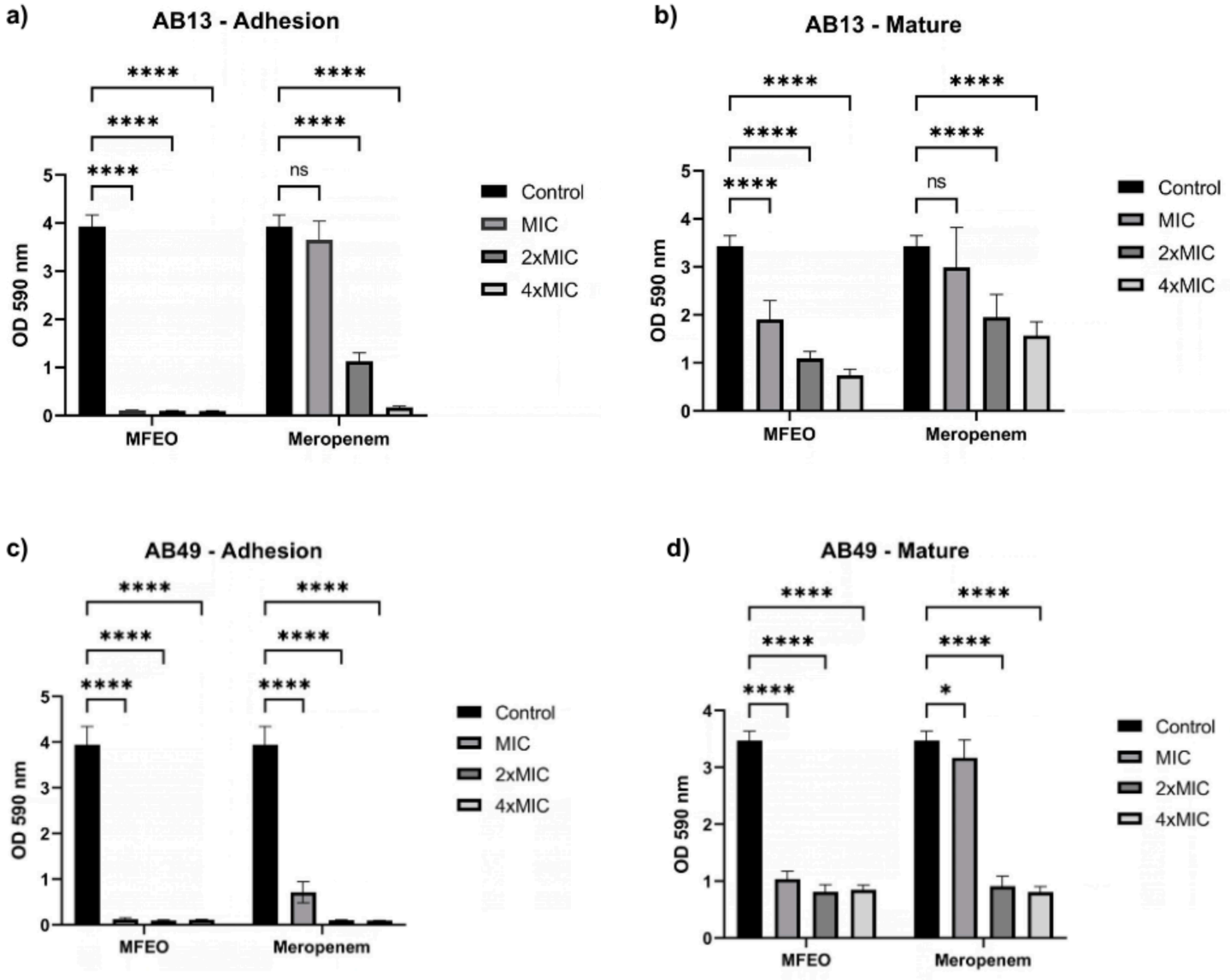


Figure 1

Effect of MFEO and meropenem on biofilm adhesion and mature biofilm of *Acinetobacter baumannii* isolates. **a** Biofilm adhesion of AB13 isolate; **b**Mature biofilm of AB13 isolate; **c** Biofilm adhesion of AB49 isolate; **d**Mature biofilm of AB49 isolate. Data represent mean ± standard deviation of three independent experiments. Asterisks indicate statistical significance (**** $p <$ 0.0001; ns: not significant). MFEO: *Monarda fistulosa*essential oil; MIC: minimum inhibitory concentration

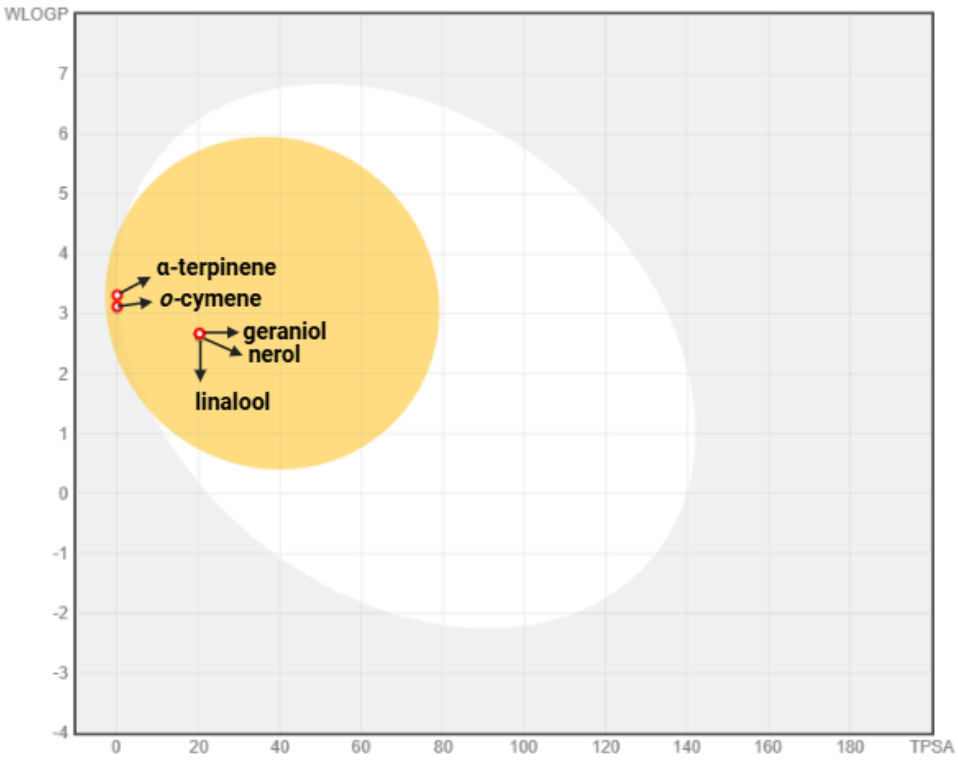


Figure 2

BOILED-Egg plot representing the gastrointestinal absorption and brain penetration of MFEO phytoconstituents

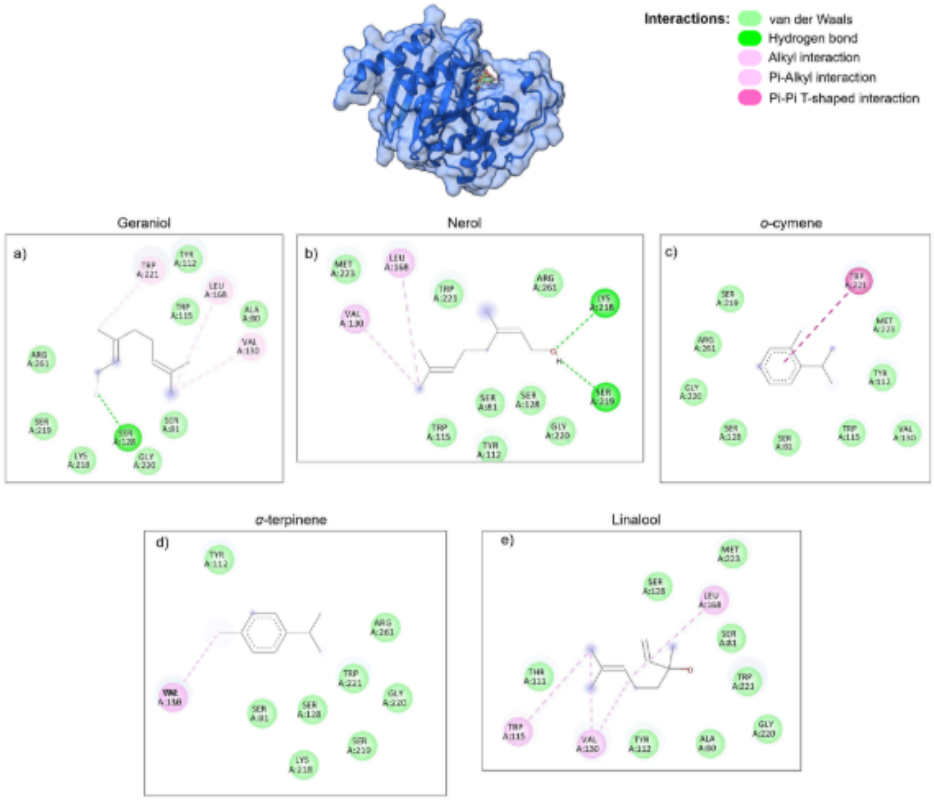


Figure 3

Main interactions between MFEO compounds and the active site of the OXA-24 carbapenemase enzyme: **a)** geraniol, **b)** nerol, **c)** linalool, **d)**α-terpinene, and **e)** *o*-cymene

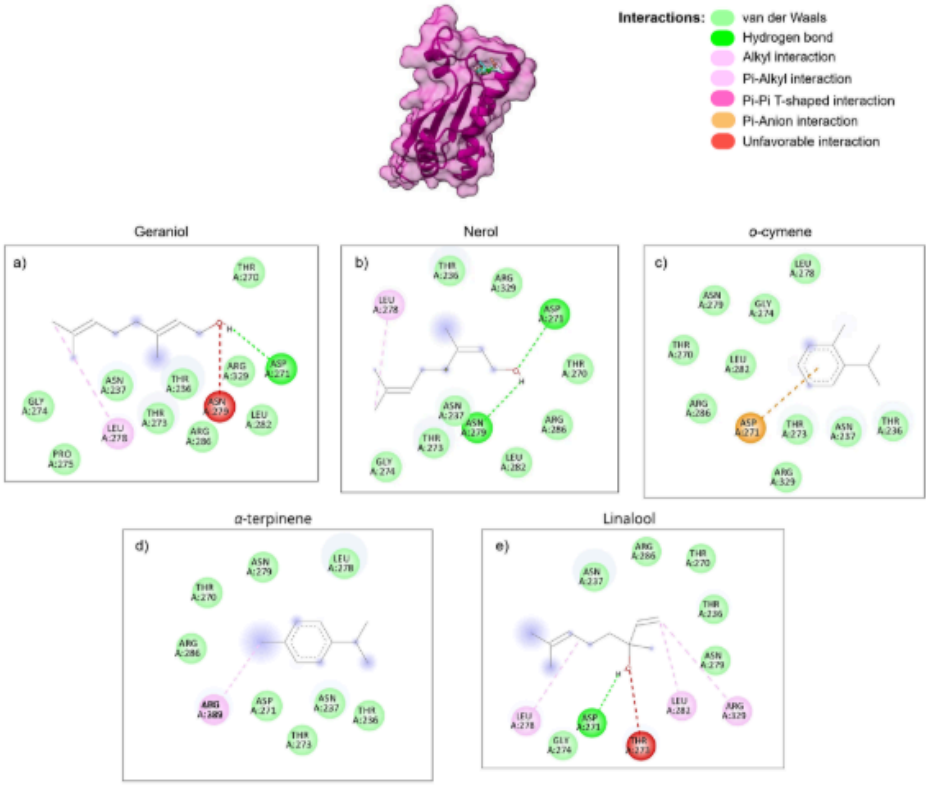


Figure 4

Main interactions between MFEO compounds and the outer membrane protein A (OmpA) of *Acinetobacter baumannii*: **a)** geraniol, **b)** nerol, **c)** linalool, **d)**α-terpinene, and **e)** *o*-cymene